Mathematical Biosciences and Engineering

http://www.aimspress.com/journal/MBE

MBE, 17(5): 5326–5340.
DOI: 10.3934/mbe.2020288
Received: 18 June 2020
Accepted: 05 August 2020
Published: 11 August 2020

Research article

Dynamics of SARS-CoV-2 infection model with two modes of transmission and immune response

Khalid Hattaf[1,2]* **and Noura Yousfi**[2]

[1] Centre Régional des Métiers de l'Education et de la Formation (CRMEF), 20340 Derb Ghalef, Casablanca, Morocco

[2] Laboratory of Analysis, Modeling and Simulation (LAMS), Faculty of Sciences Ben M'sik, Hassan II University of Casablanca, P.O Box 7955 Sidi Othman, Casablanca, Morocco

* **Correspondence:** Email: k.hattaf@yahoo.fr; Tel: +212664407825.

Abstract: In this paper, we propose a new within-host model which describes the interactions between SARS-CoV-2, host pulmonary epithelial cells and cytotoxic T lymphocyte (CTL) cells. Furthermore, the proposed model takes into account the lytic and nonlytic immune responses and also incorporates both modes of transmission that are the virus-to-cell infection through extracellular environment and the cell-to-cell transmission via virological synapses. The well-posedness of the model as well as the existence of equilibria are established rigorously. Moreover, the dynamical behaviour of the model is further examined by two threshold parameters, and the biological aspects of the analytical results are further presented.

Keywords: COVID-19; SARS-CoV-2; lytic and nonlytic immune responses; mathematical modeling; stability analysis

1. Introduction

Coronavirus disease 2019 (COVID-19) is a fatal emerging illness caused by a novel coronavirus named severe acute respiratory syndrome coronavirus 2 (SARS-CoV-2) [1]. Since the first case appeared in Wuhan of China at the end of 2019, the disease has spread quickly from country to country, provoking enormous economic damage and lot of deaths worldwide. According to the World Health Organization (WHO) report of 7 June 2020 [2], SARS-CoV-2 infected 6799713 people worldwide and caused 397388 deaths.

Recently, several mathematical models have been proposed and developed to understand the dynamics of SARS-CoV-2. However, most of these models described the propagation of the virus in human population. Therefore, the main objective of this study is to develop a within-host model that

describes the interactions between SARS-CoV-2, host pulmonary epithelial cells and cytotoxic T lymphocyte (CTL) cells. This model is governed by the following nonlinear system:

$$\begin{cases} \dfrac{dU}{dt} &= \lambda - d_U U - \dfrac{\beta_1 UV}{1+q_1 C} - \dfrac{\beta_2 UI}{1+q_2 C}, \\ \dfrac{dI}{dt} &= \dfrac{\beta_1 UV}{1+q_1 C} + \dfrac{\beta_2 UI}{1+q_2 C} - d_I I - pIC, \\ \dfrac{dV}{dt} &= kI - d_V V, \\ \dfrac{dC}{dt} &= \sigma IC - d_C C, \end{cases} \tag{1.1}$$

where $U(t)$, $I(t)$, $V(t)$ and $C(t)$ respectively indicate the concentration of uninfected pulmonary epithelial cells, infected pulmonary epithelial cells, free virus particles of SARS-CoV-2 and CTL cells at time t. Uninfected pulmonary epithelial cells are generated at a constant rate λ, die at rate $d_U U$ and become infected either by free virus particles at rate $\beta_1 UV$ or by direct contact with infected pulmonary epithelial cells at rate $\beta_2 UI$. Both modes of infection are inhibited by nonlytic immune response at rates $1 + q_1 C$ and $1 + q_2 C$, respectively. Infected pulmonary epithelial cells die at rate $d_I I$ and are killed by lytic immune response at rate pIC. The biological meanings of the remaining parameters k, d_V, σ and d_C are respectively the production rate of virus from infected pulmonary epithelial cells, the clearance rate of virus, the immune responsiveness rate, and the death rate of CTL cells. The schematic illustration of model component interactions is given in Figure 1.

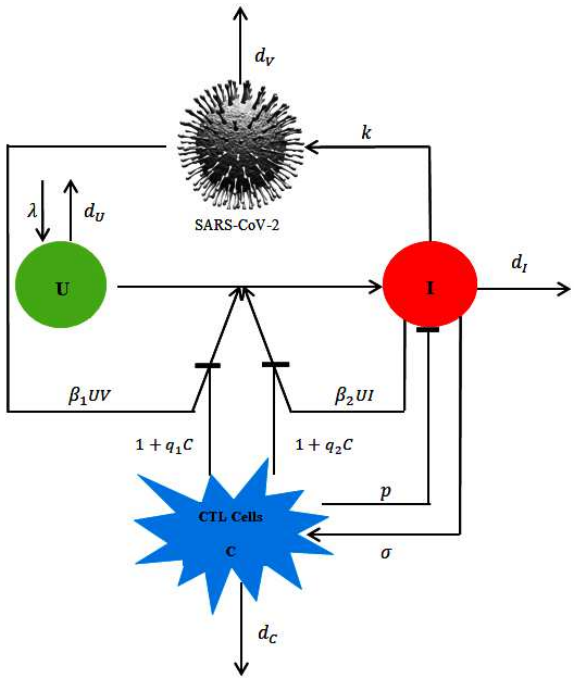

Figure 1. Schematic representation of model (1.1).

In absence of immune response, model (1.1) is reduced to

$$\begin{cases} \dfrac{dU}{dt} &= \lambda - d_U U - \beta_1 UV - \beta_2 UI, \\ \dfrac{dI}{dt} &= \beta_1 UV + \beta_2 UI - d_I I, \\ \dfrac{dV}{dt} &= kI - d_V V, \end{cases} \tag{1.2}$$

which is a special case of the model presented in [3]. Additionally, system (1.2) covers the within-host model used by Li et al. in [4] in order to estimate the parameters of SARS-CoV-2, it suffices to take $\beta_2 = 0$ and $\lambda = d_U U(0)$, where $U(0)$ is the number of uninfected epithelial cells without virus.

In presence of immune response, model (1.1) includes the following models:

- Model of Nowak and Bangham [5], when both cell-to-cell mode and nonlytic immune response are ignored, i.e., $\beta_2 = 0$ and $q_1 = 0$.
- Model of Dhar et al. [6], when the classical virus-to-cell mode is only considered.

The rest of this paper is organized in the following manner. In the next section, we establish some preliminary results about the well-posedness of the model, the existence of feasible biological equilibria and the uniform persistence of infection. In Section 3, we analyze the local and global asymptotic stability of equilibria by means of characteristic equation and Lyapunov functionals. Based on morphometric lungs data and virus environmental stability, the parameters estimation of the model is presented in Section 4. It is followed by numerical simulations in Section 5 to illustrate the obtained analytical results. The last section is devoted to the mathematical and biological conclusions drawn from this study.

2. Preliminary results

In this section, we determine some preliminary results such as the nonnegativity and boundedness of solutions in order to prove that our model (1.1) is biologically well-posed. Additionally, we establish the threshold parameters for the existence of feasible biological equilibria and we also discuss the uniform persistence of the proposed model.

Theorem 2.1. *All solutions of model (1.1) with initial conditions in $\boldsymbol{R}^4_+$ are nonnegative and bounded.*

Proof. We have

$$\begin{aligned} \frac{dU}{dt}|_{U=0} &= \lambda > 0, \\ \frac{dI}{dt}|_{I=0} &= \frac{\beta_1 UV}{1+q_1 C} \geq 0 \text{ for all } U, V, C \geq 0, \\ \frac{dV}{dt}|_{V=0} &= kI \geq 0 \text{ for all } I \geq 0, \quad \frac{dC}{dt}|_{C=0} = 0. \end{aligned}$$

This proves that $\mathbf{R}^4_+$ is positively invariant with regard to (1.1). Next, we establish the boundedness of solutions by considering the following function

$$X(t) = U(t) + I(t) + \frac{d_I}{2k} V(t) + \frac{p}{\sigma} C(t).$$

Hence,

$$\begin{aligned}\frac{dX}{dt} &= \lambda - d_U U(t) - \frac{d_I}{2} I(t) - \frac{d_I d_V}{2k} V(t) - \frac{p d_C}{\sigma} C(t) \\ &\leq \lambda - dX(t),\end{aligned}$$

where $d = \min\{d_U, \frac{d_I}{2}, d_V, d_C\}$. Thus,

$$\limsup_{t\to\infty} X(t) \leq \frac{\lambda}{d}.$$

Then $U(t)$, $I(t)$, $V(t)$ and $C(t)$ are bounded. □

Let $U_0 = \frac{\lambda}{d_U}$. Obviously, the point $P_0(U_0, 0, 0, 0)$ is the unique infection-free equilibrium (1.1). Then we define the first threshold parameter which represents the basic reproduction number of model (1.1) as follows:

$$\mathcal{R}_0 = \frac{\lambda(k\beta_1 + d_V\beta_2)}{d_U d_I d_V} = \mathcal{R}_{01} + \mathcal{R}_{02}, \tag{2.1}$$

where $\mathcal{R}_{01} = \frac{\lambda k\beta_1}{d_U d_I d_V}$ is the basic reproduction number of the classical virus-to-cell mode, while $\mathcal{R}_{02} = \frac{\lambda\beta_1}{d_U d_I}$ represents the basic reproduction number of the direct cell-to-cell mode.

In absence of immune response and $\mathcal{R}_0 > 1$, model (1.1) has another biological equilibrium called the infection equilibrium without cellular immunity labeled by $P_1(U_1, I_1, V_1, 0)$, where

$$U_1 = \frac{\lambda}{d_U\mathcal{R}_0},\ I_1 = \frac{\lambda(\mathcal{R}_0 - 1)}{d_I\mathcal{R}_0},\ V_1 = \frac{k\lambda(\mathcal{R}_0 - 1)}{d_I d_V\mathcal{R}_0}.$$

In presence of immune response, the remaining biological equilibrium of (1.1) satisfies the following equations:

$$I = \frac{d_C}{\sigma},\ V = \frac{k d_C}{\sigma d_V},\ C = \frac{\sigma(\lambda - d_U U) - d_I d_C}{p d_C} \text{ and}$$

$$\frac{k\beta_1 U}{d_V(1 + q_1 C)} + \frac{\beta_2 U}{1 + q_2 C} = d_I + pC.$$

Since $C \geq 0$, we have $U \leq \frac{\lambda}{d_U} - \frac{d_I d_C}{\sigma d_U}$. This indicates that there is no biological equilibrium when $U > \frac{\lambda}{d_U} - \frac{d_I d_C}{\sigma d_U}$ or $\frac{\lambda}{d_U} - \frac{d_I d_C}{\sigma d_U} \leq 0$. Let Y be a function defined on the closed interval $[0, \frac{\lambda}{d_U} - \frac{d_I d_C}{\sigma d_U}]$ as follows

$$Y(U) = \frac{k\beta_1 U}{d_V(1 + q_1 Z(U))} + \frac{\beta_2 U}{1 + q_2 Z(U)} - d_I - pZ(U),$$

where $Z(U) = \frac{\sigma(\lambda - d_U U) - d_I d_C}{p d_C}$. We have $Y(0) = -\frac{\sigma\lambda}{d_C} < 0$ and

$$Y'(U) = \frac{k\beta_1(1 + q_1 Z(U) - q_1 U Z'(U))}{d_V(1 + q_1 Z(U))^2} + \frac{\beta_2(1 + q_2 Z(U) - q_2 U Z'(U))}{(1 + q_2 Z(U))^2} - pZ'(U).$$

Since $Z'(U) = -\dfrac{\sigma d_U}{pd_C} < 0$, we have $Y'(U) > 0$.

When the immune response has not been established, we have from the last equation of model (1.1) that $\sigma I_1 - d_C \leq 0$. Then we define the second threshold parameter which denotes the reproduction number for cellular immunity as follows

$$\mathcal{R}_1^C = \frac{\sigma I_1}{d_C}. \tag{2.2}$$

The biological meaning of this number is given in [7]. When $\mathcal{R}_1^C < 1$, we have $I_1 < \dfrac{d_C}{\sigma}$, $U_1 > \dfrac{\lambda}{d_U} - \dfrac{d_I d_C}{\sigma d_U}$ and $Y(\dfrac{\lambda}{d_U} - \dfrac{d_I d_C}{\sigma d_U}) < \dfrac{k\beta_1 U_1}{d_V} + \beta_2 U_1 - d_I = 0$. Then there is no equilibrium when $\mathcal{R}_1^C < 1$.

When $\mathcal{R}_1^C > 1$, $I_1 > \dfrac{d_C}{\sigma}$, $U_1 < \dfrac{\lambda}{d_U} - \dfrac{d_I d_C}{\sigma d_U}$ and $Y(\dfrac{\lambda}{d_U} - \dfrac{d_I d_C}{\sigma d_U}) > 0$.

Therefore, model (1.1) has a unique infection equilibrium with cellular immunity $P_2(U_2, I_2, V_2, C_2)$, where $U_2 \in (0, \dfrac{\lambda}{d_U} - \dfrac{d_I d_C}{\sigma d_U})$, $I_2 = \dfrac{d_C}{\sigma}$, $V_2 = \dfrac{kd_C}{\sigma d_V}$ and $C_2 = \dfrac{\sigma(\lambda - d_U U_2) - d_I d_C}{pd_C}$.

By applying Theorem 4.6 in [8], we can easily obtain the following result.

Theorem 2.2. *If $\mathcal{R}_0 > 1$, then model (1.1) is uniformly persistent, i.e., there exists a positive constant ε, independent of initial conditions, such that*

$$\begin{aligned} \liminf_{t\to+\infty} U(t) &\geq \varepsilon, \quad \liminf_{t\to+\infty} I(t) \geq \varepsilon, \\ \liminf_{t\to+\infty} V(t) &\geq \varepsilon, \quad \liminf_{t\to+\infty} C(t) \geq \varepsilon. \end{aligned}$$

3. Stability analysis

This section focuses on the stability analysis of the three equilibria P_0, P_1 and P_2. The local stability is established by analyzing the characteristic equation. Whereas, the global stability is obtained by constructing favorable Lyapunov functionals.

Theorem 3.1. *The infection-free equilibrium P_0 is globally asymptotically stable if $\mathcal{R}_0 \leq 1$ and unstable if $\mathcal{R}_0 > 1$.*

Proof. Consider the following Lyapunov functional

$$L_0(U, I, V, C) = U_0 \Psi\Big(\frac{U}{U_0}\Big) + I + \frac{\beta_1 U_0}{d_V} V + \frac{p}{\sigma} C,$$

where $\Psi(x) = x - 1 - \ln x$, for $x > 0$. It is obvious that $\Psi(x) \geq 0$ for all $x > 0$, and $\Psi(x) = 0$ if and only if $x = 1$. Thus, $L_0(U, I, V, C) > 0$ for all $U, I, V, C > 0$ and $L_0(U_0, 0, 0, 0) = 0$. Further, we have

$$\begin{aligned} \frac{dL_0}{dt} &= -\frac{d_U}{U}(U - U_0)^2 + d_I I\Big(\frac{k\beta_1 U_0}{d_I d_V} + \frac{\beta_2 U_0}{d_I(1 + q_2 C)} - 1\Big) \\ &\quad -\frac{q_1 \beta_1 U_0}{1 + q_1 C} VC - \frac{pd_C}{\sigma} C \\ &\leq -\frac{d_U}{U}(U - U_0)^2 + d_I I(\mathcal{R}_0 - 1) - \frac{pd_C}{\sigma} C. \end{aligned}$$

If $\mathcal{R}_0 \leq 1$, then $\dfrac{dL_0}{dt} \leq 0$ with equality if and only if $U = U_0$, $I = 0$, $V = 0$ and $C = 0$. By applying LaSalle's invariance principle [9], we deduce that P_0 is globally asymptotically stable when $\mathcal{R}_0 \leq 1$.

If $\mathcal{R}_0 > 1$, then the characteristic equation of model (1.1) at P_0 is given by

$$(d_U + \xi)(d_C + \xi) f_0(\xi) = 0, \tag{3.1}$$

where

$$f_0(\xi) = \xi^2 + (d_I + d_V - \beta_2 U_0)\xi + d_I d_V (1 - \mathcal{R}_0).$$

We have $\lim\limits_{\xi \to +\infty} f_0(\xi) = +\infty$ and $f_0(0) = d_I d_V (1 - \mathcal{R}_0) < 0$ if $\mathcal{R}_0 > 1$. Thus, the characteristic equation (3.1) has at least one positive eigenvalue when $\mathcal{R}_0 > 1$. Then P_0 is unstable if $\mathcal{R}_0 > 1$. □

Next, we analyze the asymptotic stability of the two infection equilibria P_1 and P_2 by assuming that $\mathcal{R}_0 > 1$ and the following hypothesis

$$\begin{aligned} &q_1(C - C_i)\Big(\frac{1 + q_1 C}{1 + q_1 C_i} - \frac{V}{V_i}\Big) \leq 0, \\ &q_2(C - C_i)\Big(\frac{1 + q_2 C}{1 + q_2 C_i} - \frac{I}{I_i}\Big) \leq 0, \end{aligned} \tag{H}$$

where I_i, V_i and C_i are infected pulmonary epithelial cell, virus and CTL cell components of the infection equilibrium P_i for $i = 1, 2$.

Theorem 3.2. *Suppose that (H) holds for P_1. Then the infection equilibrium without cellular immunity P_1 is globally asymptotically stable if $\mathcal{R}_1^C \leq 1 < \mathcal{R}_0$ and unstable if $\mathcal{R}_1^C > 1$.*

Proof. Consider the following Lyapunov functional

$$L_1(U, I, V, C) = U_1 \Psi\Big(\frac{U}{U_1}\Big) + I_1 \Psi\Big(\frac{I}{I_1}\Big) + \frac{\beta_1 U_1 V_1}{k I_1} V_1 \Psi\Big(\frac{V}{V_1}\Big) + \frac{p}{\sigma} C.$$

The function Ψ was used by many authors (see for example [10–12]). By a simple computation, we find

$$\begin{aligned} \frac{dL_1}{dt} &= (1 - \frac{U_1}{U})(\lambda - d_U U) + \frac{p d_C}{\sigma}(\mathcal{R}_1^C - 1)C \\ &\quad + \beta_1 U_1 V_1 \Big(\frac{d_V V_1}{k I_1} + \frac{V}{(1 + q_1 C) V_1} - \frac{I V_1}{I_1 V} - \frac{U V I_1}{(1 + q_1 C) U_1 V_1 I}\Big) \\ &\quad + \beta_2 U_1 I_1 \Big(\frac{I}{(1 + q_2 C) I_1} - \frac{U}{(1 + q_2 C) U_1}\Big) \\ &\quad + \frac{I}{I_1}\Big(\beta_1 U_1 V_1 - d_I I_1\Big) - \frac{\beta_1 U_1 V_1}{k I_1} d_V V + d_I I_1. \end{aligned}$$

Since $\lambda = d_U U_1 + \beta_1 U_1 V_1 + \beta_2 U_1 I_1 = d_U U_1 + d_I I_1$ and $k I_1 = d_V V_1$, we have

$$\begin{aligned}\frac{dL_1}{dt} &= -\frac{d_U}{U}(U-U_1)^2+\frac{pd_C}{\sigma}(\mathcal{R}_1^C-1)C\\ &\quad+\beta_1U_1V_1\Big(3-\frac{U_1}{U}+\frac{V}{(1+q_1C)V_1}-\frac{IV_1}{I_1V}-\frac{UVI_1}{(1+q_1C)U_1V_1I}-\frac{V}{V_1}\Big)\\ &\quad+\beta_2U_1I_1\Big(2-\frac{U_1}{U}+\frac{I}{(1+q_2C)I_1}-\frac{U}{(1+q_2C)U_1}-\frac{I}{I_1}\Big).\end{aligned}$$

Hence,

$$\begin{aligned}\frac{dL_1}{dt} &= -\frac{d_U}{U}(U-U_1)^2+\frac{pd_C}{\sigma}(\mathcal{R}_1^C-1)C\\ &\quad+\beta_1U_1V_1\Big(-1-\frac{V}{V_1}+\frac{V}{(1+q_1C)V_1}+(1+q_1C)\Big)\\ &\quad+\beta_2U_1I_1\Big(-1-\frac{I}{I_1}+\frac{I}{(1+q_2C)I_1}+(1+q_2C)\Big)\\ &\quad+\beta_1U_1V_1\Big(4-\frac{U_1}{U}-\frac{IV_1}{I_1V}-\frac{UVI_1}{(1+q_1C)U_1V_1I}-(1+q_1C)\Big)\\ &\quad+\beta_2U_1I_1\Big(3-\frac{U_1}{U}-\frac{U}{(1+q_2C)U_1}-(1+q_2C)\Big).\end{aligned}$$

From (H), we have

$$\begin{aligned}-1-\tfrac{V}{V_i}+\tfrac{(1+q_1C_i)V}{(1+q_1C)V_i}+\tfrac{1+q_1C}{1+q_1C_i}&=\frac{q_1(C-C_i)}{1+q_1C}\Big(\frac{1+q_1C}{1+q_1C_i}-\frac{V}{V_i}\Big)\le 0,\\ -1-\tfrac{I}{I_i}+\tfrac{(1+q_2C_i)I}{(1+q_2C)I_i}+\tfrac{1+q_2C}{1+q_2C_i}&=\frac{q_2(C-C_i)}{1+q_2C}\Big(\frac{1+q_2C}{1+q_2C_i}-\frac{I}{I_i}\Big)\le 0.\end{aligned}\tag{3.2}$$

Since the arithmetic means (AM) is greater than or equal to the geometric mean (GM), we have

$$4-\frac{U_1}{U}-\frac{IV_1}{I_1V}-\frac{UVI_1}{(1+q_1C)U_1V_1I}-(1+q_1C)\le 0$$

and

$$3-\frac{U_1}{U}-\frac{U}{(1+q_2C)U_1}-(1+q_2C)\le 0.$$

Then if $\mathcal{R}_1^C\le 1$, we have $\dfrac{dL_1}{dt}\le 0$ with equality if and only if $U=U_1$, $I=I_1$, $V=V_1$ and $C=0$. It follows from LaSalle's invariance principle that P_1 is globally asymptotically stable when $\mathcal{R}_1^C\le 1$.

It remains to show the instability of P_1 when $\mathcal{R}_1^C>1$. The characteristic equation at this equilibrium is as follows

$$(\sigma I_1-d_C-\xi)f_1(\xi)=0,\tag{3.3}$$

where

$$f_1(\xi)=\begin{vmatrix}-d_U-\beta_1V_1-\beta_2I_1-\xi & -\beta_2U_1 & -\beta_1U_1\\ \beta_1V_1+\beta_2I_1 & \beta_2U_1-d_I-\xi & \beta_1U_1\\ 0 & k & -d_V-\xi\end{vmatrix}.$$

Then $\xi_1 = \sigma I_1 - d_C$ is a root of the characteristic equation (3.3). Since $\mathcal{R}_1^C = \frac{\sigma I_1}{d_C} > 1$, we get $\xi_1 > 0$ which implies that the characteristic equation (3.3) has a positive root when $\mathcal{R}_1^C > 1$. Thus, P_1 becomes unstable for $\mathcal{R}_1^C > 1$. This completes the proof. □

Theorem 3.3. *Suppose that (H) holds for P_2. Then the infection equilibrium with cellular immunity P_2 is globally asymptotically stable if $\mathcal{R}_1^C > 1$.*

Proof. Construct a Lyapunov functional as follows

$$L_2(U,I,V,C) = U_2\Psi\Big(\frac{U}{U_2}\Big) + I_2\Psi\Big(\frac{I}{I_2}\Big) + \frac{\beta_1 U_2 V_2}{(1+q_1C_2)kI_2}V_2\Psi\Big(\frac{V}{V_2}\Big) + \frac{p}{\sigma}C_2\Psi\Big(\frac{C}{C_2}\Big).$$

By using $\lambda = d_U U_2 + \frac{\beta_1 U_2 V_2}{1+q_1C_2} + \frac{\beta_2 U_2 I_2}{1+q_2C_2} = d_U U_2 + d_I I_2 + pI_2C_2$, $I_2 = \dfrac{d_C}{\sigma}$ and $kI_2 = d_V V_2$, we easily get

$$\begin{aligned}\frac{dL_2}{dt} &= -\frac{d_U}{U}(U-U_2)^2 \\ &\quad + \frac{\beta_1 U_2 V_2}{1+q_1C_2}\Big(3 - \frac{U_2}{U} + \frac{(1+q_1C_2)V}{(1+q_1C)V_2} - \frac{IV_2}{I_2V} - \frac{(1+q_1C_2)UVI_2}{(1+q_1C)U_2V_2I} - \frac{V}{V_2}\Big) \\ &\quad + \frac{\beta_2 U_2 I_2}{1+q_2C_2}\Big(2 - \frac{U_2}{U} + \frac{(1+q_2C_2)I}{(1+q_2C)I_2} - \frac{(1+q_2C_2)U}{(1+q_2C)U_2} - \frac{I}{I_2}\Big).\end{aligned}$$

Thus,

$$\begin{aligned}\frac{dL_2}{dt} &= -\frac{d_U}{U}(U-U_2)^2 + \frac{\beta_1 U_2 V_2}{1+q_1C_2}\Big(-1 - \frac{V}{V_2} + \frac{(1+q_1C_2)V}{(1+q_1C)V_2} + \frac{1+q_1C}{1+q_1C_2}\Big) \\ &\quad + \frac{\beta_2 U_2 I_2}{1+q_2C_2}\Big(-1 - \frac{I}{I_2} + \frac{(1+q_2C_2)I}{(1+q_2C)I_2} + \frac{1+q_2C}{1+q_2C_2}\Big) \\ &\quad + \frac{\beta_1 U_2 V_2}{1+q_1C_2}\Big(4 - \frac{U_2}{U} - \frac{IV_2}{I_2V} - \frac{(1+q_1C_2)UVI_2}{(1+q_1C)U_2V_2I} - \frac{1+q_1C}{1+q_1C_2}\Big) \\ &\quad + \frac{\beta_2 U_2 I_2}{1+q_2C_2}\Big(3 - \frac{U_2}{U} - \frac{(1+q_2C_2)U}{(1+q_2C)U_2} - \frac{1+q_2C}{1+q_2C_2}\Big).\end{aligned}$$

Since AM is greater than or equal to GM, we have

$$\begin{aligned}4 - \frac{U_2}{U} - \frac{IV_2}{I_2V} - \frac{(1+q_1C_2)UVI_2}{(1+q_1C)U_2V_2I} - \frac{1+q_1C}{1+q_1C_2} &\le 0, \\ 3 - \frac{U_2}{U} - \frac{(1+q_2C_2)U}{(1+q_2C)U_2} - \frac{1+q_2C}{1+q_2C_2} &\le 0.\end{aligned}$$

By the above and (3.2), we deduce that $\dfrac{dL_2}{dt} \le 0$ if $\mathcal{R}_1^C > 1$. It is obvious to show that $\dfrac{dL_2}{dt} = 0$ if and only if $U = U_2$, $I = I_2$, $V = V_2$ and $C = C_2$. Consequently, $\{P_2\}$ is the largest invariant subset of $\{(U,I,V,C) | \dfrac{dL_2}{dt} = 0\}$. From LaSalle's invariance principle, the steady state P_2 is globally asymptotically stable if $\mathcal{R}_1^C > 1$. □

When we ignore the nonlytic immune response, we have $q_1 = q_2 = 0$ and model (1.1) becomes

$$\begin{cases} \dfrac{dU}{dt} &= \lambda - d_U U - \beta_1 UV - \beta_2 UI, \\ \dfrac{dI}{dt} &= \beta_1 UV + \beta_2 UI - d_I I - pIC, \\ \dfrac{dV}{dt} &= kI - d_V V, \\ \dfrac{dC}{dt} &= \sigma IC - d_C C. \end{cases} \tag{3.4}$$

In this case, (H) holds. By applying Theorems 3.2 and 3.3, we have the following result.

Corollary 3.4. *Assume that $\mathcal{R}_0 > 1$.*

(i) *If $\mathcal{R}_1^C \leq 1$, then P_1 of model (3.4) is globally asymptotically stable.*

(ii) *If $\mathcal{R}_1^C > 1$, then P_1 becomes unstable and P_2 of model (3.4) is globally asymptotically stable.*

4. Parameters estimation

According to our above analytical results, model (1.1) has an unique infection-free equilibrium of the form $P_0(U_0, 0, 0, 0)$ which biologically represents the healthy state of patient without virus. Then $U_0 = \dfrac{\lambda}{d_U}$ is the total number of healthy pulmonary epithelial cells. In six adult human lungs, the mean alveolar number was 480 million with range 274–790 million, and the range of volume lungs was 2062–4744 mL [13]. For eight normal lungs [14, 15], the mean lung volume was 4341 mL with range 3500–5950 mL and the mean number of alveolar type II cells was 37 ± 5 billion. Further, the mean lung volume was estimated to be 4340 ± 285 mL in [16]. Based of the these morphometric data, we estimate $\dfrac{\lambda}{d_U}$ to be between 5.7757×10^4 and 1.2×10^7 cells/mL. However, the death rate of uninfected epithelial cells was estimated by Lee et al. [17] to be 10^{-3} day^{-1}. Therefore, we get λ between 57.757 and 1.2×10^4 cells mL^{-1} day^{-1}.

The median half-life of SARS-CoV-2 in aerosols was estimated to be between 1.1 and 1.2 hours with 95% credible interval [0.64, 2.64], it was approximately 5.6 hours on stainless steel and 6.8 hours on plastic [18]. Then we can estimate the clearance rate d_V of SARS-CoV-2 to be between 2.4464 and 15.1232 day^{-1}. It is important to note the values for d_V used in [4, 19] are included in our estimated range. For example, $d_V = 10$ day^{-1} in [19].

Based on the estimations in [4, 19, 20], we assume that the death rate of infected cells to be between 0.088 and 0.58 day^{-1}. We recall that the burst size is the mean number of virions produced by an infected cell during its lifespan. In the case of SARS-CoV-2, the burst size is unknown and was approximately estimated to be 10^3 virions [21]. Thus, we obtain k between 88 and 580 virions cell^{-1} day^{-1}. The estimation of other parameters are summarized in Table 1.

Table 1. The 12 parameters of the model (1.1) with their values.

Parameter	Definition	Value	Source
λ	Epithelial cells production rate	57.757–1.2×10^4 cells mL^{-1} day^{-1}	Calculated
d_U	Death rate of uninfected epithelial cells	10^{-3} day^{-1}	[17]
β_1	Virus-to-cell infection rate	0–1 mL virion^{-1} day^{-1}	Assumed
β_2	Cell-to-cell infection rate	0–1 mL cell^{-1} day^{-1}	Assumed
d_I	Death rate of infected epithelial cells	0.088–0.58 day^{-1}	Estimated
k	Virion production rate per infected epithelial cell	88–580 virions cell^{-1} day^{-1}	Calculated
d_V	Virus clearance rate	2.4464–15.1232 day^{-1}	Estimated
σ	Activation rate of CTL cells	0–1 mL cell^{-1} day^{-1}	Assumed
d_C	Death rate of CTL cells	0.05–1 mL cell^{-1} day^{-1}	[5]
p	Clearance rate of infection	0.05–1 mL cell^{-1} day^{-1}	[5]
q_1	Non-lytic strength against virus-to-cell infection	0–1 mL cell^{-1}	Assumed
q_2	Non-lytic strength against cell-to-cell infection	0–1 mL cell^{-1}	Assumed

5. Numerical simulations

In this section, we numerically discuss the dynamics of model (1.1) according to different parameter values.

Based on Table 1, we choose $\lambda = 500$, $d_U = 0.001$, $\beta_1 = 1.12 \times 10^{-7}$, $\beta_2 = 1.1 \times 10^{-7}$, $q_1 = 0.3$, $q_2 = 0.6$, $d_I = 0.56$, $p = 0.06$, $d_V = 10$, $d_C = 0.85$ and the other parameters σ and k are considered as free.

Case 1: When we take $\sigma = 0.05$ and $k = 88$, we have $\mathcal{R}_0 = 0.9782 \leq 1$. It follows from Theorem 3.1 that the infection-free equilibrium $P_0(5 \times 10^5, 0, 0, 0)$ is globally asymptotically stable. This theoretical result is illustrated by Figure 2 which shows the solutions of model (1.1) with different initial values tend to P_0.

Case 2: If $\sigma = 1.1 \times 10^{-3}$ and $k = 230$, then $\mathcal{R}_0 = 2.3982 > 1$ and $\mathcal{R}_1^C = 0.6737 \leq 1$. Figure 3 displays that the trajectories of model (1.1) with different initial values converge towards the infection equilibrium without cellular immunity $P_1(2.0850 \times 10^5, 520.5563, 1.1973 \times 10^4, 0)$. This confirms that P_1 is globally asymptotically stable and thus illustrates the analytical result obtained in Theorem 3.2.

Case 3: When $\sigma = 4.5 \times 10^{-3}$ and $k = 230$, we get $\mathcal{R}_0 = 2.3982 > 1$ and $\mathcal{R}_1^C = 2.7559 > 1$. In Figure 4, we observe that the trajectories of model (1.1) starting from different initial conditions tend to the infection equilibrium with cellular immunity $P_2(3.7506 \times 10^5, 188.2088, 4.3292 \times 10^3, 1.6977)$. This validates the global asymptotic stable of P_2 given in Theorem 3.3.

From the explicit formula of the basic reproduction number of $\mathcal{R}_0$ given in (2.1), we see that $\mathcal{R}_0$ is an increasing function with respect to k and it does not depend on σ. Also, the second threshold parameter $\mathcal{R}_1^C$ is a increasing function with respect to k and σ (see, Figure 5).

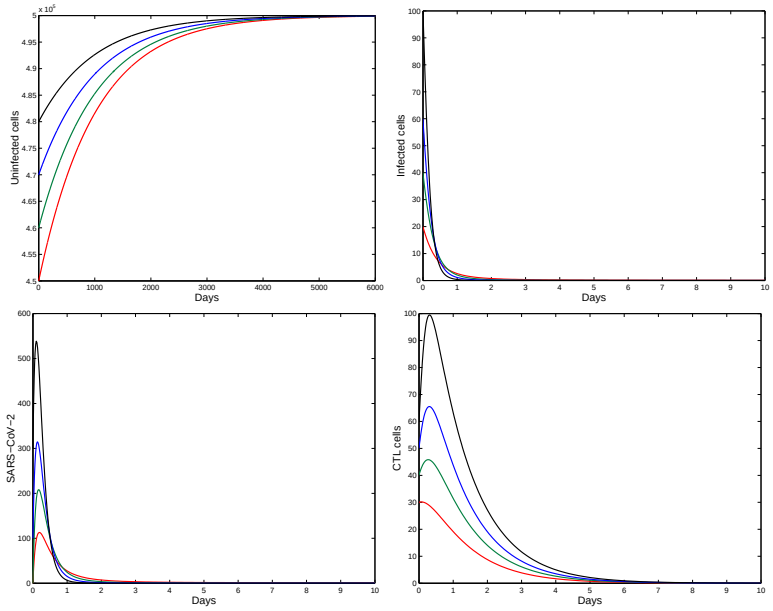

Figure 2. Dynamics of model (1.1) when $\mathcal{R}_0 = 0.9782 \leq 1$.

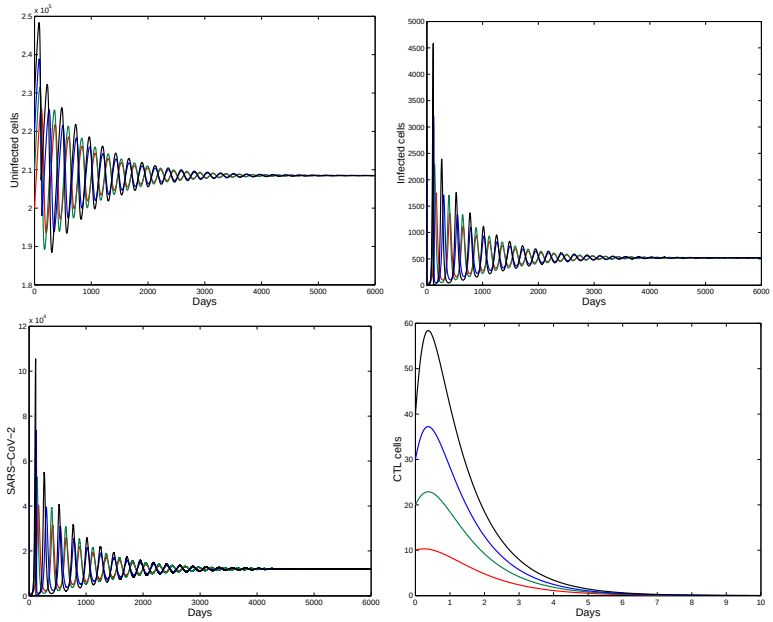

Figure 3. Dynamics of model (1.1) when $\mathcal{R}_0 = 2.3982 > 1$ and $\mathcal{R}_1^C = 0.6737 \leq 1$.

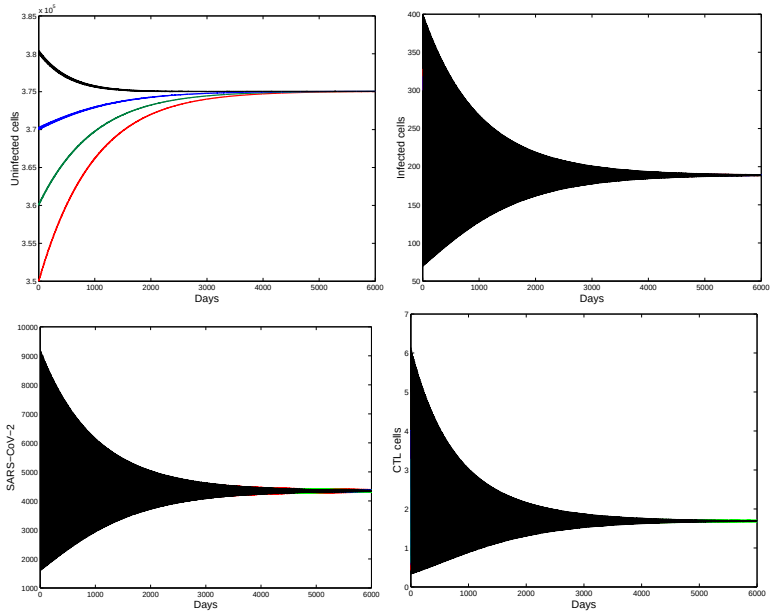

Figure 4. Dynamics of model (1.1) when $\mathcal{R}_0 = 2.3982 > 1$ and $\mathcal{R}_1^C = 2.7559 > 1$.

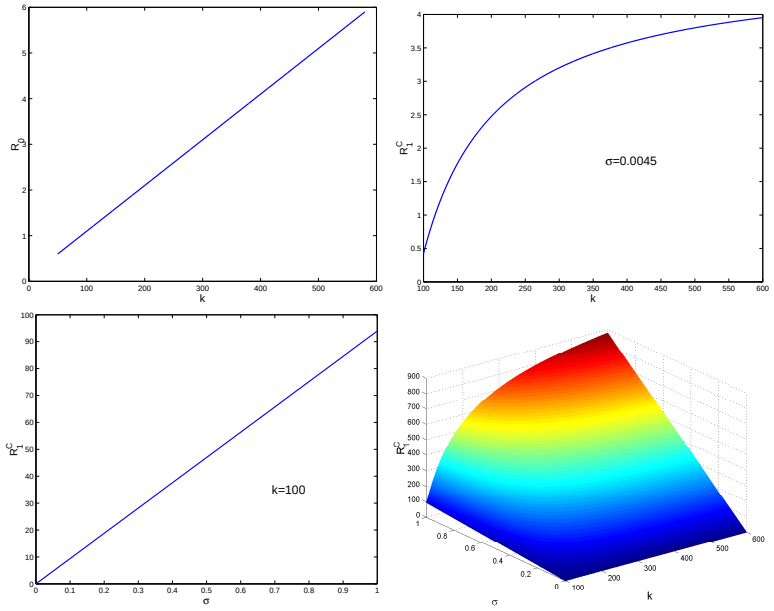

Figure 5. Plot showing the relationship of k and σ with the two reproduction numbers $\mathcal{R}_0$ and $\mathcal{R}_1^C$.

6. Discussion and conclusion

In this article, we have proposed a new mathematical model to better describe the dynamics of COVID-19 in human body with virus-to-cell infection, cell-to-cell transmission, lytic and nonlytic

immune responses. We have first provided the result regarding the well-posedness of the proposed model in terms of nonnegativity and boundedness of the solutions. Investigating for the biologically feasible equilibria of this SARS-CoV-2 infection model, we have obtained two threshold parameters which completely determine the dynamics of the model. The first threshold parameter called the basic reproduction number labeled by $\mathcal{R}_0$ and the second is the reproduction number for cellular immunity denoted by $\mathcal{R}_1^C$. We have proved in Theorem 2.2 that the proposed model is uniformly persistent when $\mathcal{R}_0 > 1$, which biologically means that the SARS-CoV-2 persists in the host when $\mathcal{R}_0 > 1$. Further, our analytical results suggest that the infection-free equilibrium P_0 is globally asymptotically stable whenever $\mathcal{R}_0 \leq 1$ (see, Theorem 3.1). This means the complete eradication of SARS-CoV-2 in human lungs. From our numerical results, this eradication of the virus and the extinction of the infection can be done after five days (see, Figure 2). However, P_0 becomes unstable when $\mathcal{R}_0 > 1$ and two scenarios arise depending on the value of the reproduction number for cellular immunity $\mathcal{R}_1^C$. When $\mathcal{R}_1^C \leq 1$, the infection equilibrium without cellular immunity P_1 is globally asymptotically stable (see, Theorem 3.2). This indicates that the immune response has not been established, which causes persistence of SARS-CoV-2 in human lungs. When $\mathcal{R}_1^C > 1$, P_1 becomes unstable and the infection equilibrium with cellular immunity P_2 is globally asymptotically stable (see, Theorem 3.3). In this case, the virus is also persisted in the lungs because of the weak response of cellular immunity (see, Figure 4). Furthermore, we have estimated some parameters of the model based on morphometric data and virus environmental stability.

Currently, there is no licensed drug or vaccine against COVID-19. The results of this study establish new within-host properties of SARS-CoV-2 and they can help the biologists and pharmaceutical companies to develop an effective treatment for COVID-19 that makes the patient's basic reproduction number $\mathcal{R}_0$ less than or equal to one, which automatically lead to the eradication of SARS-CoV-2 from the patient's lungs. Since $\mathcal{R}_0$ is the sum of the basic reproduction numbers for the virus-to-cell and cell-to-cell transmission modes, the last direct mode of transmission should not be ignored in the dynamics of SARS-CoV-2 infection so as not to underestimate the value of the basic reproduction number.

Acknowledgements

We would like to thank the editor and anonymous reviewers for their constructive comments and suggestions, which have improved the quality of the manuscript.

Conflict of interest

There is no conflicts of interest.

References

1. A. E. Gorbalenya, S. C. Baker, R. S. Baric, R. J. de Groot, C. Drosten, A. A. Gulyaeva, et al., The species severe acute respiratory syndromerelated coronavirus: classifying 2019-nCoV and naming it SARS-CoV-2, *Nat. Microbiol.*, **5** (2020), 536.

2. WHO, *Coronavirus disease 2019 (COVID-19)*, Situation Report-139, 2020. Available from: https://www.who.int/docs/default-source/coronaviruse/situation-reports/20200607-covid-19-sitrep-139.
3. K. Hattaf, N. Yousfi, Qualitative analysis of a generalized virus dynamics model with both modes of transmission and distributed delays, *Int. J. Differ. Equations*, **2018** (2018), 1–7.
4. C. Li, J. Xu, J. Liu, Y. Zhou, The within-host viral kinetics of SARS-CoV-2, *Math. Biosci. Eng.*, **17** (2020), 2853–2861.
5. M. A. Nowak, C. R. Bangham, Population dynamics of immune responses to persistent viruses, *Science*, **272** (1996), 74–79.
6. M. Dhar, S. Samaddar, P. Bhattacharya, R. K. Upadhyay, Viral dynamic model with cellular immune response: A case study of HIV-1 infected humanized mice, *Physica A*, **524** (2019), 1–14.
7. K. Hattaf, Spatiotemporal dynamics of a generalized viral infection model with distributed delays and CTL immune response, *Computation*, **7** (2019), 1–16.
8. H. R. Thieme, Persistence under relaxed point-dissipativity (with application to an endemic model), *SIAM J. Math. Anal.*, **24** (1993), 407–435.
9. J. P. LaSalle, *The Stability of Dynamical Systems, Regional Conference Series in Applied Mathematics*, SIAM Philadelphia, 1976.
10. P. Roop-O, W. Chinviriyasit, S. Chinviriyasit, The effect of incidence function in backward bifurcation for malaria model with temporary immunity, *Math. Biosci.*, **265** (2015), 47–64.
11. C. Yang, X. Wang, D. Gao and J. Wang, Impact of awareness programs on Cholera dynamics: Two modeling approaches, *Bull. Math. Biol.*, **79** (2017), 2109–2131.
12. K. Hattaf, Global stability and Hopf bifurcation of a generalized viral infection model with multi-delays and humoral immunity, *Physica A*, **545** (2020), 123689.
13. M. Ochs, J. R. Nyengaard, A. Jung, L. Knudsen, M. Voigt, T. Wahlers, J. Richter, H. G. Gundersen, The number of alveoli in the human lung, *Am. J. Respir. Crit. Care Med.*, **169** (2004), 120–124.
14. P. Gehr, M. Bachofen, E. R. Weibel, The normal human lung: ultrastructure and morphometric estimation of diffusion capacity, *Resp. Physiol.*, **32** (1978), 121–140.
15. J. D. Crapo, B. E. Barry, P. Gehr, M. Bachofen, E. R. Weibel, Cell number and cell characteristics of the normal human lung, *Am. Rev. Respir. Dis.*, **126** (1982), 332–337.
16. E. R. Weibel, What makes a good lung? The morphometric basis of lung function, *Swiss Med. Wkly.*, **139** (2009), 375–386.
17. H. Y. Lee, D. J. Topham, S. Y. Park, J. Hollenbaugh, J. Treanor, T. R Mosmann, et al., Simulation and prediction of the adaptive immune response to influenza A virus infection, *J. Virol.*, **83** (2009), 7151–7165.
18. N. van Doremalen, T. Bushmaker, D. H. Morris, M. G. Holbrook, A. Gamble, B. N. Williamson, et al., Aerosol and surface stability of SARS-CoV-2 as compared with SARS-CoV-1, *N. Engl. J. Med.*, **382** (2020), 1564–1567.

19. P. Czuppon, F. Débarre, A. Goncalves, O. Tenaillon, A. S. Perelson, J. Guedj, et al., Predicted success of prophylactic antiviral therapy to block or delay SARS-CoV-2 infection depends on the targeted mechanism, *MedRxiv*, (2020).
20. A. Gonçalves, J. Bertrand, R. Ke, E. Comets, X. de Lamballerie, D. Malvy, et al., Timing of antiviral treatment initiation is critical to reduce SARS-Cov-2 viral load, *MedRxiv*, (2020).
21. Y. M. Bar-On, A. Flamholz, R. Phillips, R. Milo, Science Forum: SARS-CoV-2 (COVID-19) by the numbers, *Elife*, **9** (2020), e57309.